as a mercury sensor.[12–15] Although data suggesting Hg^{II}-recognition have been reported,[16–28] no definitive conclusion had been made regarding the recognition mode of Hg^{II} until our previous study.[15] The above mentioned DNA duplexes, which include metal-mediated base pairs, could be potentially useful for nanotechnology devices because of the controllability of the secondary and tertiary structures of the DNA molecules.[29,30]

NMR spectroscopy is a suitable method for investigating the physicochemical properties of a DNA duplex with T-Hg^{II}-T pairs, because it provides structural information on target molecules and their solution equilibria.[13–15,25–28,31–36] Therefore, here we carried out NMR spectroscopic studies on the complex formed by Hg^{II} and a DNA duplex, d(CGCG**TT**GTCC) • d(GGAC**TT**CGCG), since, within the sequences we examined, this duplex gave the most clear spectra. This is the first NMR study of the DNA duplex containing consecutive metal ions.

EXPERIMENTAL SECTION

Sample Preparation

Two DNA decamers, 5′-CGCGTTGTCC-3′ and 5′-GGACTTCGCG-3′, were synthesized by using a phosphoramidite method on an automated DNA/RNA synthesizer model 392 (Applied Bio-systems, Foster City, CA). Each oligomer was purified on a C18 reverse-phase column (Cosmosil 5C18-AR-300; Nakalai Tesque, Kyoto, Japan) in a high performance liquid chromatography (HPLC) system, with a linear gradient of 5–50% acetonitrile (30 min), 0.1M triethylammonium acetate as a basal buffer, and a flow rate of 3.0 mL/min. For the exchange of counter ions, each oligomer was adsorbed onto an anion-exchange column (UNO-Q; BIO-RAD, Hercules, CA). The column was washed with more than 10 column volumes of Milli-Q water (Millipore, Billerica, MA) to wash out the triethylammonium ions. The oligomer was then eluted with 2M NaCl so that Na^+ became the counter ion. Finally, excess NaCl was removed by desalting on a gel filtration column (TSK-GEL G3000PW; TOSOH, Tokyo, Japan) with Milli-Q water as the mobile phase. The final solution contained only the oligomer and the counter ion (Na^+). Each oligomer was quantitated by ultraviolet (UV) absorbance at 260 nm after digestion with nuclease P1.

Titration Experiments with UV Spectra

UV spectra were recorded for a solution containing 5 μM of the DNA duplex (d(CGCGTTGTCC) • d(GGACTTCGCG)), 20 mM Na-MOPS buffer (pH 7.0), in the presence of various concentrations of $Hg(OAc)_2$. UV absorbances at 275 nm were plotted against the molar equivalents.

Two-Dimensional NMR Measurements

Typical solutions for two-dimensional (2D) NMR measurements contained 2.0 mM DNA duplex, 100 mM $NaClO_4$, 1.0 mM Na-cacodylate buffer pH 6.0, with or without 4.8 mM $Hg(ClO_4)_2$, in D_2O. Two-dimensional ^1H-^1H NOESY spectrum without $Hg(ClO_4)_2$ were recorded on a JEOL ECA600 spectrometer, at 296 K, with 2048 * 1024 complex points for a spectral width of 5402 * 5402 Hz, and 16 scans were averaged. Two-dimensional ^1H-^1H COSY spectrum without $Hg(ClO_4)_2$ was recorded on a JEOL ECA600 spectrometer, at 296 K, with 1024 * 1024 complex points for a spectral width of 5402 * 5402 Hz, and 16 scans were averaged. We used an absolute value COSY spectrum for the mercury-free duplex due to a severe cross-peak overlap. Two-dimensional ^1H-^1H NOESY spectrum with $Hg(ClO_4)_2$ was recorded on a Bruker DRX800 spectrometer, at 293 K, with 8192 * 2048 complex points for a spectral width of 8013 * 8013 Hz, and 16 scans were averaged. Phase-sensitive ^1H-^1H COSY spectrum with $Hg(ClO_4)_2$ was recorded on a Bruker DRX800 spectrometer, at 296 K, with 8192 * 1024 complex points for a spectral width of 8013 * 8013 Hz, and 16 scans were averaged.

Titration Experiments with NMR Spectra

Solutions for 1D ^1H NMR measurements contained 2.0 mM DNA duplex, 100 mM $NaClO_4$, 2.0 mM Na-cacodylate buffer (pH 6.0), and various concentrations of $Hg(ClO_4)_2$ in H_2O/D_2O (95:5). We selected an Na-cacodylate system as a buffer, since cacodylate does not precipitate with Hg^{II} under the conditions that we used. In spite of the buffer usage, pH became approximately 4 at the final titration point. However, we confirmed that spectral patterns of the di-mercurated DNA oligomers at pH 4 was essentially the same as those at pH 6. Titration experiments with 1D ^1H NMR spectra were recorded on a JEOL ECA600 spectrometer, at 296 K, with 32,768 complex points for a spectral width of 15,024 Hz, and processed using an exponential function to give line broadening of 3 Hz.

RESULTS AND DISCUSSION

Titration Experiments with UV Spectra

In order to confirm whether the synthesized DNA duplex was suitable for titration experiments with NMR spectra, we examined the affinity of Hg^{II} for the DNA duplex and determined how many Hg^{II} were able to bind to the DNA duplex. For this purpose, we performed titration experiments of the DNA duplex with Hg^{II}, by using UV absorbances at 275 nm (Figure 1). It was found that the titration curve was sharply kinked at 2 molar equivalents of Hg^{II} to a DNA duplex, indicating that 2 molar equivalents of Hg^{II} bound

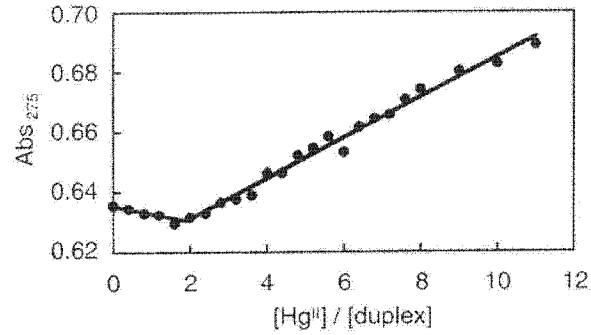

FIGURE 1 Plot of UV absorbances at 275 nm against molar equivalents ([Hg^{II}] / [duplex]). Least-squares fitted lines are shown. Possible explanations for the UV absorbance changes might be due to changes in the spectral intensity of thymidines themselves upon mercuration (0–2 eq.)[15] and putative non-specific interactions of Hg^{II} with DNA oligomers (2–11 eq.).[19,20] Titration NMR spectra also suggested this non-specific binding, since the methyl proton resonance of T8 in di-mercurated DNA duplex (white star) shifted most extensively during titrations, although T8 was not a mercurated site (Figure 4).

to one DNA duplex. This finding is plausible because the DNA duplex contained two T-T mismatches (the putative Hg^{II}-binding site) per duplex. More importantly, the sharp kink in the titration curve indicated that the concentrations of Hg^{II} and the DNA duplex were much higher than the *Kd* value for the Hg^{II}-DNA complexation, indicating that Hg^{II} had very high affinity for this DNA duplex. Therefore, the DNA duplex used here is suitable for physicochemical studies such as structural and thermodynamic studies.

Resonance Assignments for the Mercury-Free DNA Duplex

Before the titration experiments, resonance assignments of the DNA duplex d(CGCGTTGTCC) • d(GGACTTCGCG) needed to be carried out. Therefore, we recorded 2D ^{1}H-^{1}H NOESY and 2D ^{1}H-^{1}H COSY spectra for the duplex in D_2O (Figure 2). In the cross section between H8/H6/H2 and H1′/H5, H5-H6 correlations of cytidines were identified from the COSY spectrum (Figure 2b). Due to a severe cross-peak overlap, we used a conventional absolute value COSY spectrum (Figure 2b). With reference to this information, we were able to assign all base protons and anomeric protons. It was found that sequential NOE walks between base protons and anomeric protons could be traced though both strands (Figure 2a).

We next extended these assignments to other sugar proton resonances, with reference to the abovementioned assignments. In the cross section between base protons and H2′/H2″, their sequential NOE walks were traceable through both strands. H3′ and H4′ resonances were assigned by using the NOE cross-peaks with intra-residue H1′ resonances.[37] Stereo-specific assignments of H2′/H2″ resonances were performed by using cross-peak intensities of H2′-H3′ and H2″-H3′, estimated from the COSY spectrum.[37] Methyl proton resonances (Me) of thymidines were assigned by using intra-residue H6-Me NOE cross-peaks. Finally, H5′ and H5″ resonances were assigned by

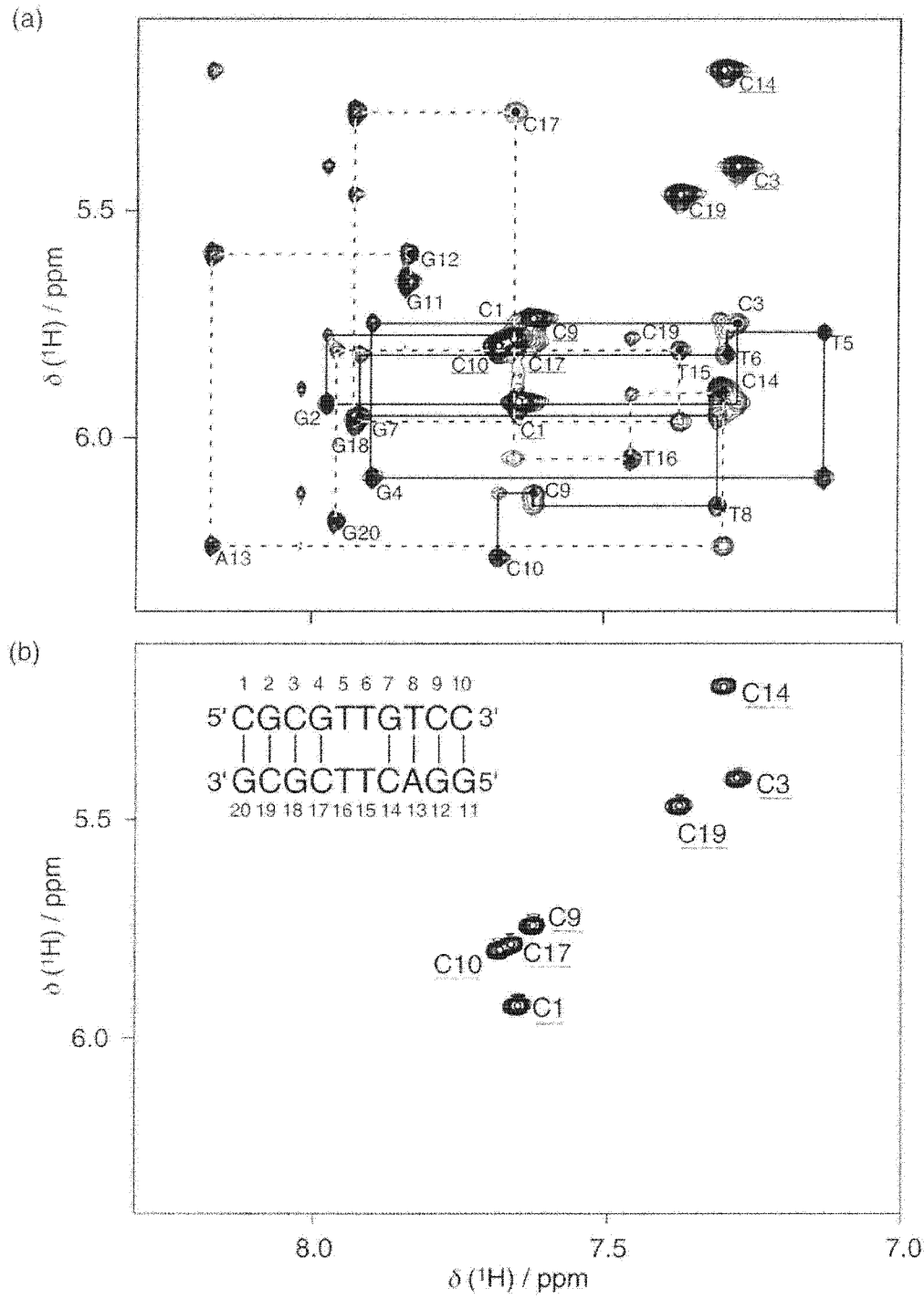

FIGURE 2 NOESY and absolute value COSY spectra for the mercury-free DNA duplex. (a) NOESY spectrum with sequential NOE walks between anomeric (H1′) and base protons (black line: C1-C10; dotted line: G11-G20). Intra-residue cross-peaks are presented with the corresponding residue numbers (closed circles). (b) COSY spectrum with H5-H6 cross-peaks of cytidines labeled with their residue numbers.

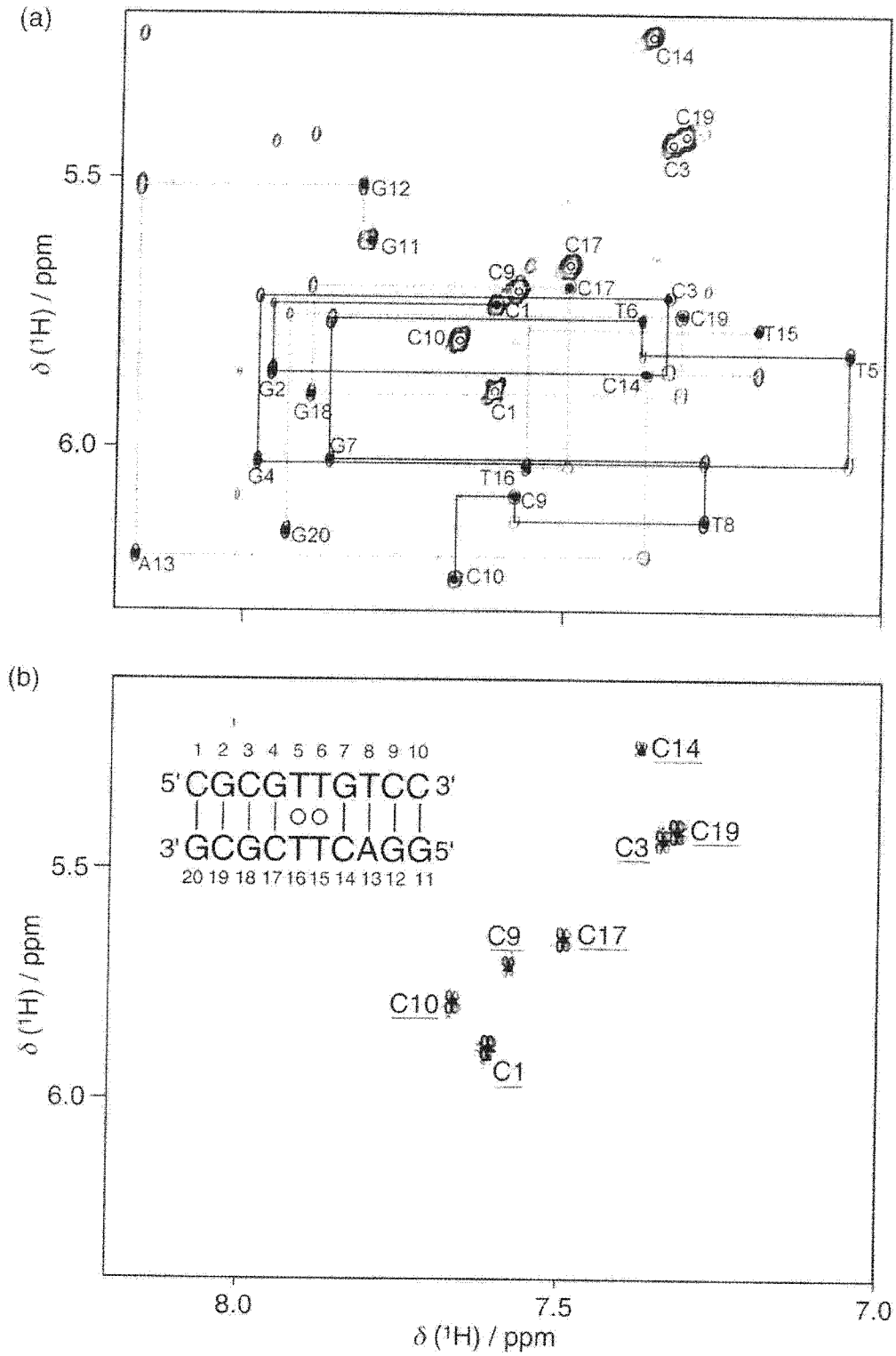

FIGURE 3 NOESY and phase-sensitive COSY spectra for the di-mercurated DNA duplex. (a) NOESY spectrum with sequential NOE walks between anomeric (H1′) and base protons (black line: C1-C10, dotted line: G11-G20). Intra-residue cross-peaks are presented with the corresponding residue numbers (closed circles). (b) COSY spectrum with H5-H6 cross-peaks of cytidines labeled with their residue numbers.

TABLE 1 Chemical Shift Table for the Mercury-Free DNA Duplex[a]

	H2/H5/Me[b]	H6/H8[c]	H1′	H2′	H2″	H3′	H4′	H5′/H5″[d]
C1	5.93	7.65	5.78	2.00	2.47	4.72	4.08	3.75/3.75
G2	n.a.	7.98	5.93	2.69	2.75	4.98	4.37	4.01/3.73
C3	5.41	7.28	5.75	1.92	2.40	4.85	4.20	4.15/4.10
G4	n.a.	7.90	6.09	2.66	2.78	4.95	4.41	4.13/4.10
T5	1.66	7.13	5.77	1.96	2.47	4.76	4.15	4.40/4.13
T6	1.54	7.30	5.84	2.04	2.44	4.84	4.15	-/-
G7	n.a.	7.92	5.95	2.63	2.79	4.94	4.33	4.12/4.09
T8	1.35	7.31	6.15	2.21	2.57	4.91	4.27	4.24/4.18
C9	5.74	7.62	6.12	2.24	2.52	4.86	4.20	4.24/4.15
C10	5.80	7.68	6.26	2.30	2.30	4.58	4.06	4.20/4.18
G11	n.a.	7.85	5.66	2.48	2.67	4.82	4.17	3.67/3.67
G12	n.a.	7.83	5.60	2.69	2.77	5.02	4.38	-/-
A13	8.02	8.17	6.24	2.69	2.86	5.04	4.49	4.25/4.21
C14	5.20	7.31	5.90	2.25	2.49	4.68	4.30	4.09/-
T15	1.65	7.31	5.91	1.95	2.43	4.74	4.06	4.21/-
T16	1.50	7.46	6.05	2.01	2.43	4.82	4.05	4.17/-
G17	5.78	7.66	5.29	2.38	2.43	4.89	4.19	4.04/3.99
G18	n.a.	7.93	5.97	2.61	2.73	5.02	4.37	3.99/-
C19	5.47	7.37	5.84	1.97	2.38	4.86	4.19	4.21/4.15
G20	n.a.	7.96	6.19	2.64	2.39	4.70	4.21	4.10/-

[a] Chemical shifts are given in ppm.

[b] Chemical shifts for H2 of adenosine, or H5 of cytidine, or the methyl proton of thymidine.

[c] Chemical shifts for H8 of the purine residues or H6 of the pyrimidine residues.

[d] Chemical shifts for H5′ and H5″. Stereospecific assignments were not carried out.

n.a.: not applicable (Assignments were not applicable due to the lack of the corresponding protons.) -: not assigned, due to signal overlaps.

using the residual NOE cross-peaks with base protons. Thus, we assigned 164 nonexchangeable proton resonances out of 173 expected resonances (Table 1). These assignments were fully consistent within the NOESY and COSY spectra.

Resonance Assignments for the Di-Mercurated DNA Duplex

Next, we performed resonance assignments for the Hg^{II}-DNA (2:1) complex as described for the mercury-free complex above, except that the phase-sensitive COSY spectrum was used. The NOESY and COSY spectra are presented in Figure 3. Basically, resonance assignments were performed as described above. In addition, by using the phase-sensitive COSY spectrum, *J*-coupling values for H1′-H2′/H2″ could be read. Therefore, stereospecific assignments of H2′ and H2″ resonances were performed with reference to these *J*-coupling values, in combination with the H3′-H2′/H2″ cross-peak in the COSY spectrum (data not shown).[37] The resulting resonance assignments are listed in Table 2. Thus, we assigned all 173 expected resonances

TABLE 2 Chemical Shift Table for the Di-Mercurated DNA Duplex[a]

	H2/H5/Me[b]	H6/H8[c]	H1′	H2′	H2″	H3′	H4′	H5′/H5″[d]
C1	5.89	7.61	5.74	1.94	2.38	4.69	4.05	3.70/3.70
G2	n.a.	7.96	5.86	2.66	2.69	4.96	4.33	3.96/4.07
C3	5.44	7.34	5.72	2.01	2.43	4.85	4.18	4.13/4.18
G4	n.a.	7.98	6.03	2.58	2.82	4.95	4.39	4.09/4.12
T5	1.56	7.06	5.82	1.89	2.51	4.75	4.12	4.09/4.27
T6	1.80	7.38	5.76	2.22	2.27	4.82	3.99	4.08/4.10
G7	n.a.	7.87	6.02	2.64	2.81	4.92	4.35	3.97/4.08
T8	1.26	7.28	6.14	2.20	2.54	4.90	4.23	4.15/4.17
C9	5.71	7.58	6.09	2.21	2.48	4.82	4.16	4.05/4.11
C10	5.80	7.67	6.24	2.27	2.27	4.56	4.04	3.93/4.15
G11	n.a.	7.81	5.62	2.45	2.62	4.79	4.13	3.62/3.62
G12	n.a.	7.82	5.52	2.67	2.73	4.99	4.34	4.02/4.10
A13	8.01	8.17	6.20	2.66	2.84	5.03	4.46	4.16/4.21
C14	5.24	7.38	5.86	2.29	2.50	4.67	4.28	4.07/4.23
T15	1.72	7.20	5.78	1.72	2.27	4.62	3.92	4.01/4.23
T16	1.64	7.56	6.03	2.25	2.50	4.84	4.16	3.91/3.98
C17	5.66	7.50	5.70	2.11	2.38	4.82	4.08	4.10/4.21
G18	n.a.	7.90	5.90	2.61	2.71	4.97	4.34	4.00/4.10
C19	5.42	7.32	5.76	1.90	2.32	4.81	4.15	4.07/4.09
G20	n.a.	7.94	6.15	2.36	2.61	4.67	4.17	4.05/4.04

[a]Chemical shifts are given in ppm.

[b]Chemical shifts for H2 of adenosine, or H5 of cytidine, or the methyl proton of thymidine.

[c]Chemical shifts for H8 of the purine residues or H6 of the pyrimidine residues.

[d]Chemical shifts for H5′ and H5″. Stereospecific assignments were not carried out.

n.a.: not applicable (Assignments were not applicable due to the lack of the corresponding protons.)

(Table 2). We confirmed that these assignments were consistent within the NOESY and COSY spectra.

From NOESY spectra in the presence (Figure 3a) and absence (Figure 2a) of Hg^{II}, the DNA oligomers were found to be in a duplex form, irrespective of whether the DNA oligomers captured Hg^{II} or not. This is because sequential NOE walks were traceable through the strands in both conditions (Figures 2a and 3a).

Titration Experiments with NMR Spectra

We have already reported the results of primitive titration experiments of this DNA duplex with Hg^{II},[15] performed with reference to imino proton resonances, which were directly exchanged with Hg^{II}. From these experiments, we were able to monitor the direct exchange of imino protons of T-T mismatches with Hg^{II}.[15] However, in order to detect each duplex species (mercury-free, mono-mercurated and di-mercurated DNA duplexes), resonances of non-exchangeable protons (i.e., methyl protons) are superior to those of imino protons (exchangeable protons), because exchangeable

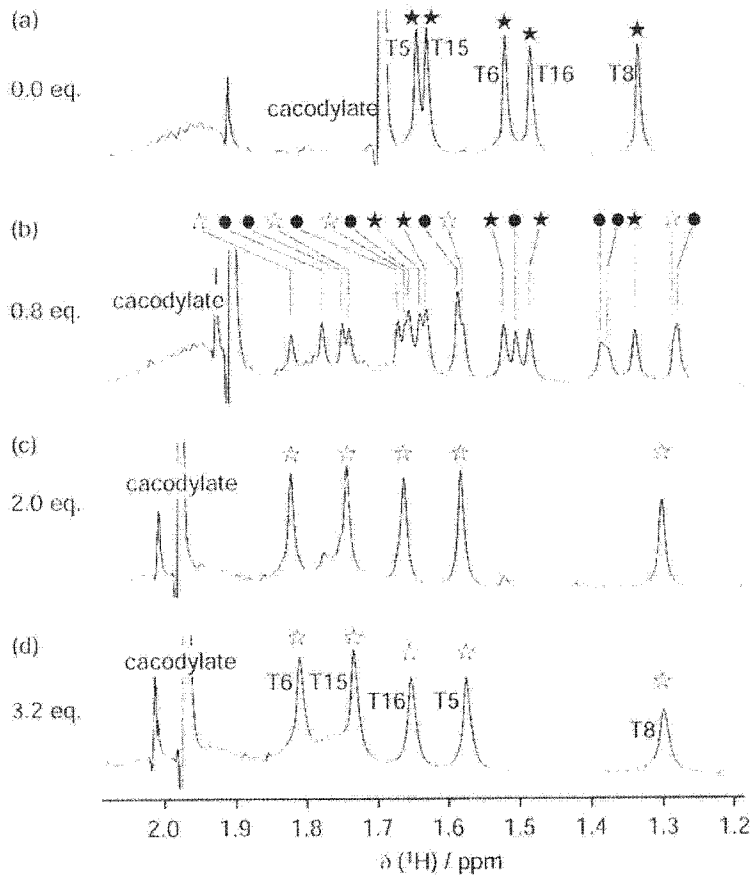

FIGURE 4 Titration experiments using 1D ^{1}H NMR spectra. Molar equivalents ([Hg^{II}]/[duplex]) are presented on the left of each panel. Resonance assignments for methyl protons of thymidines in the mercury-free and di-mercurated duplexes are presented in the top and bottom panels, respectively. Resonances are labeled with black stars (mercury-free duplex), black circles (mono-mercurated duplex), or white stars (di-mercurated duplex), with respect to their origins. Small minor peaks in panel (c) were not assigned currently.[38] Slight signal broadening under Hg^{II}-excess conditions is found to be due to a contamination of trace amount of para-magnetic metal ions in the $Hg(ClO_4)_2$ reagent.

proton resonances often disappear due to chemical exchanges during structural transitions.

Therefore, we monitored methyl proton resonances of thymidines in the presence of various concentrations of $Hg(ClO_4)_2$ (Figure 4). This is because methyl proton resonances are observed in a region that is independent from other resonances and T-T mismatches are the target sites for Hg^{II}. From the titration spectra, it was found that most duplexes were converted into the di-mercurated species with 2 molar equivalents of Hg^{II} to the duplex (Figure 4c).[38] This observation is consistent with the results of titration experiments using UV spectra (Figure 1). During the course of the titrations, independent signals from mercury-free and di-mercurated DNA duplex species were observed simultaneously (Figure 4b). More interestingly, in addition to these signals, we observed unassigned signals other than those from the mercury-free and di-mercurated species (Figure 4b). This is a clear

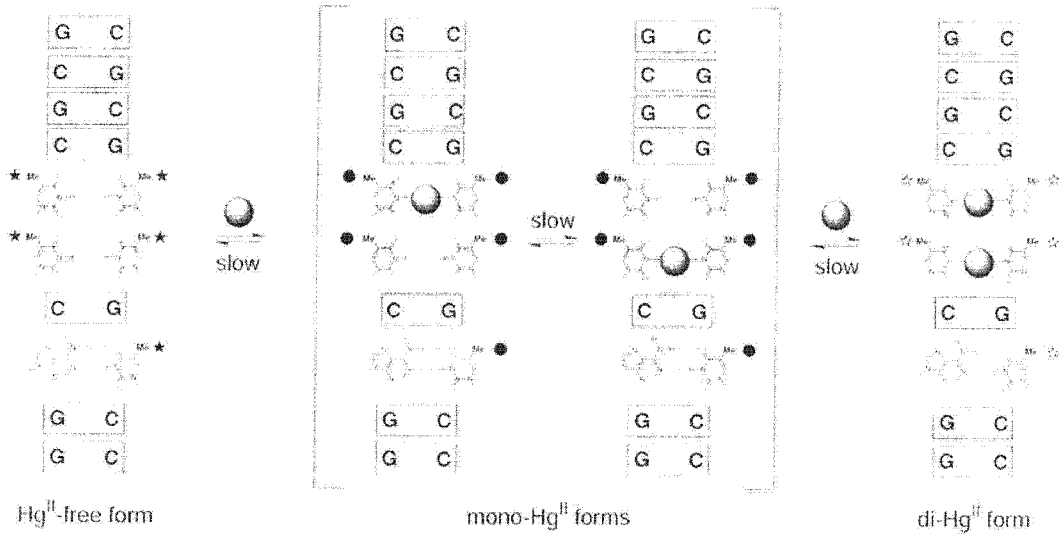

FIGURE 5 Equilibrium system of mercury-free, mono-mercurated and di-mercurated duplexes. Methyl groups are labeled with black stars (mercury-free duplex), black circles (mono-mercurated duplex), or white stars (di-mercurated duplex), as shown in Figure 4.

indication of the existence of transient species. Furthermore, this indicates that the Hg^{II}-association and dissociation processes were so slow that individual species in solution gave independent signals. Thus, this DNA duplex-Hg^{II} complex is an interesting system for the physicochemical studies of nucleic acid-metal complexations, because of the observation of transient species.

A possible candidate for the transient species is two DNA duplexes in complex with a single Hg^{II} at one of the T-T mismatches (Figure 5). If this is the case, there would be two mono-Hg^{II} species and, in total, four species of DNA duplexes possible, namely one Hg^{II}-free form, two mono-Hg^{II} forms and one di-Hg^{II} form (Figure 5). Therefore, 20 methyl proton signals should be observed (four species each with five methyl groups) under Hg^{II}-unsaturated conditions. At least 19 signals were identified at 0.8 molar equivalents of Hg^{II} to one DNA duplex (Figure 4b). It should also be mentioned that we could easily identified the ^1H resonances of the transient species because of the rigid assignments of methyl proton resonances of the mercury-free and di-mercurated DNA duplexes. Consequently, we unambiguously determined the existence of a transient species, and were able to account for the NMR spectra based on the structural transition between mercury-free, mono-mercurated and di-mercurated DNA duplexes. In our previous paper, we observed transient signals of imino protons, as well.[15] Accordingly, it was reconfirmed that these transient signals of imino protons arose from two kinds of mono-Hg^{II} species.

CONCLUDING REMARKS

We performed NOE-based resonance assignments for the mercury-free and di-mercurated DNA duplexes, and assigned most of the

non-exchangeable proton resonances except for several H5′/H5″ resonances. Then, we performed titration experiments using 1D ^{1}H NMR spectra and found that the Hg^{II} association and dissociation processes were so slow that species in solution gave independent ^{1}H resonances. Because of the resonance assignments of the mercury-free and di-mercurated species, we could unambiguously identify ^{1}H resonances from transient species, most likely two mono-mercurated species. The titration NMR spectra were consistent with the structural transitions between the mercury-free, mono-mercurated and di-mercurated DNA duplexes.

REFERENCES

1. Meggers, E.; Holland, P.L.; Tolman, W.B.; Romesberg, F.E.; Schultz, P.G. A novel copper-mediated DNA base pair. Journal of the American Chemical Society **2000**, 122, 10714–10715.
2. Atwell, S.; Meggers, E.; Spraggon, G.; Schultz, P.G. Structure of a copper-mediated base pair in DNA. Journal of the American Chemical Society **2001**, 123, 12364–12367.
3. Zimmermann, N.; Meggers, E.; Schultz, P.G. A novel silver(I)-mediated DNA base pair. Journal of the American Chemical Society **2002**, 124, 13684–13685.
4. Zimmermann, N.; Meggers, E.; Schultz, P.G. A second-generation copper(II)-mediated metallo-DNA-base pair. Bioorganic Chemistry **2004**, 32, 12–25.
5. Zhang, L.; Meggers E. An extremely stable and orthogonal DNA base pair with a simplified three-carbon backbone. Journal of the American Chemical Society **2005**, 127, 74–75.
6. Weizman, H.; Tor, Y. 2,2′-Bipyridine ligandoside: A novel building block for modifying DNA with intra-duplex metal complexes. Journal of the American Chemical Society **2001**, 123, 3375–3376.
7. Tanaka, K.; Yamada, Y.; Shionoya, M. Formation of silver(I)-mediated DNA duplex and triplex through an alternative base pair of pyridine nucleobases. Journal of the American Chemical Society **2002**, 124, 8802–8803.
8. Tanaka, K.; Tengeiji, A.; Kato, T.; Toyama, N.; Shiro, M.; Shionoya, M. Abstract Efficient incorporation of a copper hydroxypyridone base pair in DNA. Journal of the American Chemical Society **2002**, 124, 12494–12498.
9. Tanaka, K.; Tengeiji, A.; Kato, T.; Toyama, N.; Shionoya, M. A discrete self-assembled metal array in artificial DNA. Science **2003**, 299, 1212–1213.
10. Switzer, C.; Shin D. A pyrimidine-like nickel(II) DNA base pair. Chemical Communications **2005**, 1342–1344.
11. Switzer, C.; Sinha, S.; Kim, P.H.; and Heuberger, B.D. A purine-like nickel(II) base pair for DNA. Angewandte Chemie International Edition **2005**, 44, 1529–1532.
12. Ono A.; Togashi H. Highly selective oligonucleotide-based sensor for mercury(II) in aqueous solutions. Angewandte Chemie International Edition **2004**, 43, 4300–4302.
13. Yamaguchi, H.; Oda, S.; Kondo, Y.; Ono, A.; Tanaka, Y. Spectroscopic analysis of DNA duplexes including T-T mismatches. Nucleic Acids Symposium Series **2004**, 48, 113–114.
14. Yamaguchi, H.; Oda, S.; Kojima, C.; Ono, A.; Kondo, Y.; Tanaka, Y. Spectroscopic analyses of DNA duplexes in the presence of mercury ions. Nucleic Acids Symposium Series **2005**, 49, 199–200.
15. Miyake, Y.; Togashi, H.; Tashiro, M.; Yamaguchi, H.; Oda, S.; Kudo, M.; Tanaka, Y.; Kondo, Y.; Sawa, R.; Fujimoto, T.; Machinami, T.; and Ono, A. Mercury^{II} mediated formation of thymine-Hg^{II}-thymine base pairs in DNA duplexes. Journal of the American Chemical Society **2006**, 128, 2172–2173.
16. Yamane, T.; Davidson, N. 1961. On the Complexing of Desoxyribonucleic Acid (DNA) by Mercuric Ion. Journal of the American Chemical Society **1961**, 83, 2599–2607.
17. Katz, S. Reversible reaction of double-stranded polynucleotides and Hg^{II}: Separation of the strands. Nature **1962**, 195, 997–998.
18. Katz, S. The reversible reaction of Hg(II) and double-stranded polynucleotides. A step-function theory and its significance. Biochimica et Biophysica Acta **1963**, 68, 240–253.
19. Simpson, R.B. Association Constants of Methylmercuric and Mercuric Ions with Nucleosides. Journal of the American Chemical Society **1964**, 86, 2059–2065.

20. Izatt, R.M.; Christensen, J.J; Rytting, J.H. Sites and thermodynamic quantities associated with proton and metal ion interaction with ribonucleic acid, deoxyribonucleic acid, and their constituent bases, nucleosides, and nucleotides. Chemical Review **1971**, 71, 439–481.
21. Kosturko, L.D.; Folzer, C.; Stewart, R.F. The crystal and molecular structure of a 2:1 complex of 1-methylthymine-mercury(II). Biochemistry **1974**, 13, 3949–3952.
22. Gruenwedel, D.W.; Cruikshank M.K. Mercury-induced DNA polymorphism: Probing the conformation of Hg(II)-DNA via staphylococcal nuclease digestion and circular dichroism measurements. Biochemistry **1990**, 29, 2110–2116.
23. Gruenwedel, D.W. Effect of Hg(II) on the spectroscopic properties of poly[d(A-T)•d(A-T)] and poly[d(A)•d(T)] and their constituent subunits (deoxyadenosine and thymidine monomers and dimers). Biophysical Chemistry **1994**, 52, 115–123.
24. Gruenwedel, D.W. Effect of Hg(II) on the spectroscopic properties of DNA bases: Circular dichroism of deoxyadenosine and thymidine monomers and dimers. Journal of Inorganic Biochemistry **1994**, 56, 201–212.
25. Onvido, I.; Norris, A.R.; Buncel, E. Biomolecule-mercury interactions: Modalities of DNA base-mercury binding mechanisms. Remediation strategies. Chemical Reviews **2004**, 104, 5911–5929.
26. Buncel, E.; Boone, C.; Joly, H.; Kumar, R.; Norris, A.R.J. Metal ion-biomolecule interactions 12. ^{1}H and ^{13}C NMR evidence for the preferred reaction of thymidine over guanosine in exchange and competition reactions with mercury(II) and methylmercury(II). Inorganic Biochemistry **1985**, 25, 61–73.
27. Buncel, E.; Boone, C.; Joly, H. Metal ion-biomolecule interactions 13. NMR evidence for the Formation of the mixed-ligand thymidine-mercury-guanosine complex—a model for a putative Hg(II) interstrand cross-linking structure of DNA. Inorganic Chimica Acta **1986**, 125, 167–172.
28. Kuklenvik Z.; Marzilli L.G. Mercury(II) Site-Selective Binding to a DNA Hairpin. Relationship of Sequence-Dependent Intra- and Interstrand Cross-Linking to the Hairpin-Duplex Conformational Transition. Inorganic Chemistry **1996**, 35, 5654–5662.
29. Seeman, N.C. DNA in a material world. Nature **2003**, 421, 427–431.
30. Mao, C.; Sun, W.; Shen, Z.; Seeman, N.C. A nanomechanical device based on the B-Z transition of DNA. Nature **1999**, 397, 144–146.
31. Tanaka, Y.; Taira, K. Detection of RNA nucleobase metalation by NMR spectroscopy. Chemical Communications **2005**, 2069–2079.
32. Tanaka, Y.; Kasai, Y.; Mochizuki, S.; Wakisaka, A.; Morita, E.H.; Kojima, C.; Tooyozawa, A.; Kondo, Y.; Taki, M.; Takagi, Y.; Inoue, A.; Yamasaki, K.; Taira, K. Nature of the chemical bond formed with the structural metal ion at the A9–G10.1 motif derived from hammerhead ribozymes. Journal of the American Chemical Society **2004**, 126, 714–732.
33. Tanaka, Y.; Kojima, C.; Morita, E.H.; Kasai, Y.; Yamasaki, K.; Ono, A.; Kainosho M.; Taira, K. Identification of the metal ion binding site on an RNA motif from hammerhead ribozymes using ^{15}N NMR spectroscopy. Journal of the American Chemical Society **2002**, 124, 4595–4601.
34. Suzumura, K.; Yoshinari, K.; Tanaka, Y.; Takagi, Y.; Kasai, Y.; Warashina, M.; Kuwabara, T.; Orita, M.; Taira, K. A reappraisal, based on ^{31}P NMR, of the direct coordination of a metal ion with the phosphoryl oxygen at the cleavage site of a hammerhead ribozyme. Journal of the American Chemical Society **2002**, 124, 8230–8236.
35. Tanaka, Y.; Morita, E.H.; Hayashi, Y.; Kasai, Y.; Tanaka T.; Taira, K. Well-conserved tandem G•A pairs and the flanking C•G pair in hammerhead ribozymes are sufficient for capture of structurally and catalytically important metal ions. Journal of the American Chemical Society **2000**, 122, 11303–11310.
36. Tanaka, Y.; Kojima, C.; Yamazaki, T.; Kodama, T.S.; Yasuno, K.; Miyashita, S.; Ono, A.; Ono, A.; Kainosho, M.; Kyogoku, Y. Solution structure of an RNA duplex including a C-U base pair. Biochemistry **2000**, 39, 7074–7080.
37. Wüthrich, K. *NMR of Proteins and Nucleic Acids*. John Wiley & Sons: New York **1986**.
38. In Figure 4c, unassigned small signals were observed, and there are two possibilities for this result. One is the possibility that the unassigned signals are those from a transient species, and other signals of the transient species are overlapped with those from dimercurated species. The other is that unassigned signals arise from an unknown minor conformer. Currently, we can not determine which hypothesis is plausible.
39. Thomas, G.A. The Interaction of Hg(II) with Sodium Thymonucleate. Journal of the American Chemical Society **1954**, 76, 6032–6034.

Journal of Biomolecular NMR (2006) 36:69

Letter to the Editor

^{1}H, ^{13}C and ^{15}N resonance assignments of the VAP-A: OSBP complex

DOI 10.1007/s10858-006-9057-2

The 25-hydroxycholesterol (25-OHC) traffic by oxysterol binding protein (OSBP) is mediated by complex formation of OSBP with VAMP-associated protein-A (VAP-A). VAP-A is an endoplasmic reticulum (ER) integral membrane protein that contains a cytoplasmic major sperm protein (MSP) domain. There is a FFAT (referring to two phenylalanines [FF] in an acidic tract) motif in OSBP that is recognized by the MSP domain of VAP-A. Thus, the interaction facilitates localization of OSBP to the ER, where newly synthesized 25-hydroxycholesterol (25-OHC) efficiently binds to OSBP (Wyles et al., 2002). As a first step toward understanding the mechanism of 25-OHC traffic mediated by VAP-A and OSBP, we performed NMR studies of the complex composed of a VAP-A MSP domain (5–128) and an OSBP peptide (345–379) containing the FFAT motif. 2D, 3D and 4D NMR experiments were performed with the complex composed of ^{13}C- and ^{15}N-labeled VAP-A and non-labeled OSBP, ^{13}C- and ^{15}N-labeled OSBP and non-labeled VAP-A, and ^{15}N-labeled VAP-A and ^{15}N-labeled OSBP. All resonances of the backbone nuclei (^{1}HN, ^{15}N, $^{13}C\alpha$ and $^{13}C'$) of the complex were assigned with the exception of N34 C' of VAP-A. Furthermore, more than 90% of the side chain ^{1}H and ^{13}C resonances of the complex were also assigned. T367-G373 of OSBP showed minor peaks possibly derived from a minor conformation. BMRB deposit with accession No. 7025.
Reference: Wyles et al. (2002) *J. Biol. Chem.*, **277**, 29908–29918.

Kyoko Furuita, Masaki Mishima & Chojiro Kojima*
Graduate School of Biological Sciences, Nara Institute of Science and Technology, 8916-5 Takayama, Ikoma 630-0192, Japan

*To whom correspondence should be addressed. E-mail: kojima@bs.naist.jp
Supplementary material is available to authorised users in the online version of this article at http://dx.doi.org/10.1007/s10858-006-9057-2.

Nucleic Acids Symposium Series No. 50 47–48
doi:10.1093/nass/nrl024

Structural analyses on the mercury^{II}-mediated T-T base pair

Yoshiyuki Tanaka[1], Shuji Oda[1], Hiroshi Yamaguchi[1], Megumi Kudo[1], Yoshinori Kondo[1], Chojiro Kojima[2] and Akira Ono[3]

[1]Graduate School of Pharmaceutical Sciences, Tohoku University, Aobayama, Aoba-ku, Sendai 980-8578, Japan, [2]Graduate School of Sciences, NAIST, Ikoma 630-0101, Japan and [3]Department of Material and Life Chemistry, Faculty of Engineering, Kanagawa University, Yokohama 221-8686, Japan

ABSTRACT

Recently, it was reported that T-T mismatches can specifically recognize Hg^{II}, and form T-Hg^{II}-T pairs. In order to understand the structure and properties of the T-Hg^{II}-T pair, we measured NMR spectra for a DNA duplex, d(CGCGTTGTCC) • d(GGACTTCGCG), with two successive T-T mismatches (Hg^{II}-binding sites) in the middle of the duplex. We identified imino proton resonances of the T-T mismatches in mercury-free duplex, and performed titration experiments with Hg^{II} by using 1-dimensional (1D) ^{1}H NMR spectra. From the titration spectra, disappearances of imino proton signals were observed upon the addition of Hg^{II}. Furthermore, we observed additional signals of transient species, most likely mono-mercurated duplexes. This is an evidence that structural transformations between Hg^{II}-free and Hg^{II}-bound forms are slow enough for each species to give independent signals. These data strongly suggest that the imino protons of thymine bases were substituted with Hg^{II}, to form T-Hg^{II}-T pairs in which one Hg^{II} cross-links two N3 atoms of thymines.

INTRODUCTION

Nucleic acid-metal interactions are interesting target to be solved, because they are related to folding of nucleic acids, mechanism of actions of ribonucleic acid enzymes (ribozymes), mutations of genes (for example Hg^{2+}-induced mutation) and designs of biomolecular devices with metal cofactors[1]. Among these topics, metal-mediated base pairs with "artificial" nucleobases are extensively studied for nano-devices and tools for biotechnology[2-5]. On the other hand, we have reported that a "natural" base, thymine-thymine (T-T) mismatch in a DNA duplex, specifically bound to Hg^{II}[6-8]. According to the reports in the 1960s and later, protons are released when Hg^{II} binds to thymine residues in DNA[9-17]. Then, Katz proposed the formation of mercury-thymine (1:2) complexes[10]. Although data suggesting Hg^{II}-recognition mode have been reported as shown above[10,13-17], no definitive conclusion had been made regarding the recognition mode of Hg^{II} (the chemical structure of T-Hg^{II}-T pair). In addition, the overall structure of a DNA duplex with T- Hg^{II}-T pairs remains unknown. Therefore, here we analyzed this proton- Hg^{II} exchanging processes upon the T-Hg^{II}-T pairing by means of NMR spectroscopy.

RESULTS AND DISCUSSION

For the chemical structure analysis of the T-Hg^{II}-T pair, we thought that proton-Hg^{II} exchanging process must be observed. In order to confirm the dissociation of the imino protons of thymine residues upon the formation of T-Hg^{II}-T pairs, titration experiments of a DNA duplex with Hg^{II} were performed. Among the sequences we examined, the duplex 5'-CGCGTTGTCC-3' • 5'-GGACTTCGCG-3' (two T-T mismatches are in the middle) gave the most clearly interpreted spectrum. In the absence of Hg^{II}, four imino proton signals of the T-T mismatches (10.4~11.1 ppm) were observed, in conjunction with those of the Watson-Crick base pairs (12.5~13.5 ppm) (Figure 1). However, upon the addition of 2.0 molar equivalents of Hg^{II}, the imino proton resonances of the T-T mismatches almost disappeared (Figure 1), which suggests that the imino protons of the T-T mismatches in the Hg^{II}-free duplex were substituted with Hg^{II} ions.

Interestingly, the imino proton signals from putative transient species (most likely mono-mercurated DNA duplexes) were observed separately from a non-mercurated DNA duplex, under Hg^{II}-unsaturated conditions (Figure 1c). This unambiguously indicates that the Hg^{II} association and dissociation processes occur slowly relative to the NMR time scale. As a result, all the exchanging processes should occur slowly, including those between water protons and imino protons. Accordingly, the disappearances of imino proton signals could be attributed to the dissociation of imino protons from thymine residues. In other word, it was strongly suggested that Hg^{II} binds directly to N3 of thymidine in place of the imino proton, which leads to the formation of the T-Hg^{II}-T pair (Figure 1a).

As one of possible explanations for the above phenomena, imino proton signals of T-T mismatches might be observed from a non-mercurated species and two kinds of mono-mercurated species, independently (Figure 1e). If we assume that Hg^{II}-binding occurs through the equilibrium system as shown in Figure 1e, eight imino proton signals should be observed. This is because the non-mercurated species gives four signals (filled circles in Figure 1), two kinds of mono-mercurated species give four signals (two signals from each species: filled stars in Figure 1), and the

di-mercurated species does not give any imino proton signal due to proton-Hg^{II} exchanges. In fact, eight expected imino proton signals were observed (Figures 1b-d). In addition, similar phenomena were observed for the methyl proton signals of thymidines[8]. In the methyl proton region, 20 kinds of methyl proton signals were observed against 20 expected signals under Hg^{II}-unsaturated conditions (five methyl groups in each duplex (four kinds of species))[8]. Therefore, all the ^1H NMR spectral data support that Hg^{II}-binding occurs through the equilibrium system as shown in Figure 1e.

For more definitive conclusion on the structure of Hg^{II}-mediated T-T pairs, ^{15}N NMR spectroscopy and NOE-based solution structure determinations are underway.

CONCLUSION

It was found that the exchange rate between Hg^{II}-free and Hg^{II}-bound states for the duplex: 5'-CGCGTTGTCC-3' • 5'-GGACTTCGCG-3' were slow, and proton signals from each state was independently observed. Accordingly, the disappearances of imino proton signals could be attributed to the proton-Hg^{II} exchanges upon the formation of Hg^{II}-mediated T-T pair.

REFERENCES

1. Lippard, S.J., Berg, J.M. (1996) *Principles of Bioinorganic Chemistry*, University Science Books, California.
2. Meggers, E., Holland, P.L., Tolman, W.B., Romesberg, F.E., Schultz, P. G. (2000) *J. Am. Chem. Soc.*, **122**, 10714-10715.
3. Weizman, H., Tor, Y. (2001) *J. Am. Chem. Soc.*, **123**, 3375-3376.
4. Tanaka, K., Tengeiji, A., Kato, T., Toyama, N., Shionoya, M. (2003) *Science*, **299**, 1212-1213.
5. Switzer, C., Sinha, S., Kim, P.H., Heuberger, B.D. (2005) *Angew. Chem. Int. Ed.*, **44**, 1529-1532.
6. Ono, A., Togashi, H. (2004) *Angew. Chem. Int. Ed. Engl.*, *43* (**33**), 4300-4302.
7. Miyake, Y., Togashi, H., Tashiro, M., Yamaguchi, H., Oda, S., Kudo, M., Tanaka, Y., Kondo, Y., Sawa, R., Fujimoto, T., Machinami, T., Ono, A. (2006) *J. Am. Chem. Soc.*,**128**, 2172-2173.
8. Tanaka, Y., Yamaguchi, H., Oda, S., Nomura, M., Kojima, C., Kondo, Y., Ono, A. (2006) *Nucleosides Nucleotides & Nucleic Acid*, **25**, 613-624.
9. Yamane, T., Davidson, N. (1961) *J. Am. Chem. Soc.*, **83**, 2599-2607.
10. Katz S. (1963) *Biochim. Biophys. Acta.*, **68**, 240-253.
11. Simpson, R.B. (1964) *J. Am. Chem. Soc.*, **86**, 2059-2065.
12. Izatt, R.M., Christensen, J.J, Rytting, J.H. (1971) *Chem. Rev.*, **71**, 439-481.
13. Kosturko, L.D., Folzer, C., Stewart, R.F. (1974) *Biochemistry*, **13**, 3949-3952.
14. Gruenwedel, D.W., Cruikshank M.K. (1990) *Biochemistry*, **29**, 2110-2116.
15. Buncel, E., Boone, C., Joly, H., Kumar, R., Norris, A. R.J. (1985) *Inorg. Biochem.*, **25**, 61-73.
16. Buncel, E., Boone, C., Joly, H. (1986) *Inorg. Chem. Acta - Bioinorg. Chem.*, **125**, 167-172.
17. Kuklenyik, Z., Marzilli, L.G. (1996) *Inorg. Chem.*, **35**, 5654-5662.

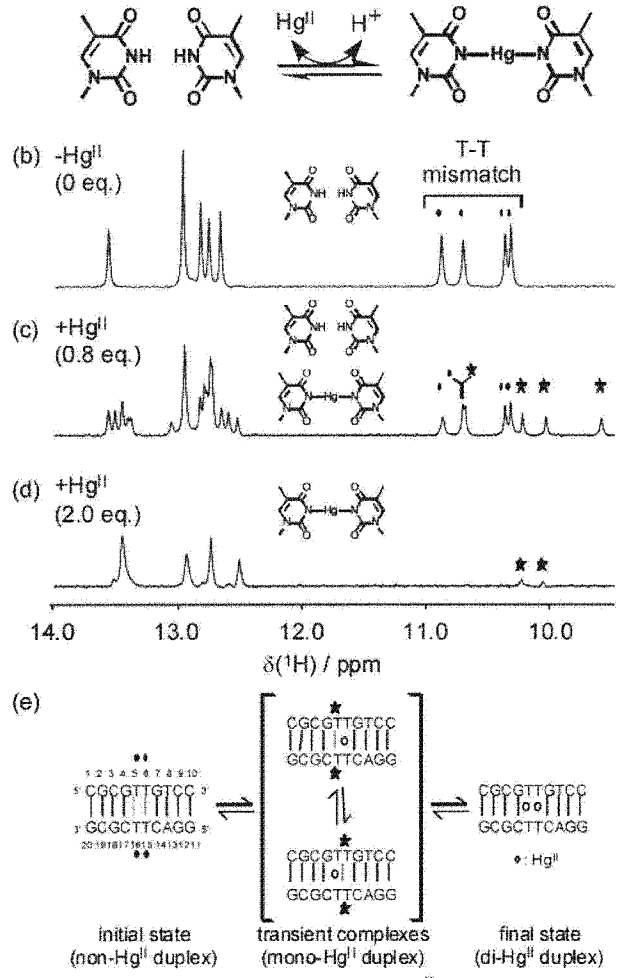

Figure 1 Putative chemical structure of Hg^{II}-mediated T-T pair, titration NMR spectra, and equilibrium system during titrations.

Nucleic Acids Symposium Series No. 50 259–260
doi:10.1093/nass/nrl129

Studies of DNA recognition mechanism of transcription factor IRF-4

Kyoko Furuita[1], Itsuko Ishizaki[1], Harumi Fukada[2], Kazuo Yamamoto[3], Toshifumi Matsuyama[3], Makoto Nomura[1], Masaki Mishima[1] and Chojiro Kojima[1]

[1]Laboratory of Biophysics, Graduate School of Biological Sciences, Nara Institute of Science and Technology, 8916-5 Takayama, Ikoma, Nara 630-0192, Japan, [2]Laboratory of Biophysical Chemistry, Graduate School of Life and Environmental Sciences, Osaka Prefecture University, 1-1 Gakuen-cho,Nakaku,Sakai,Osaka 599-8531, Japan and [3]Division of Cytokine Signaling, Department of Molecular Microbiology and Immunology, Nagasaki University Graduate School of Biomedical Sciences, 1-12-4 Sakamoto, Nagasaki 852-8523, Japan

ABSTRACT

Transcription factor IFN regulatory factor-4 (IRF-4) prefers a DNA sequence including CCGAAA, though the consensus DNA-binding sequence of the IRF family proteins is NNGAAA, and the crystal structure of PU.1/IRF-4/DNA (GTGAAA) ternary complex indicates the NN region of DNA does not interact with IRF-4 directly. This suggests that there is an indirect DNA recognition mechanism in IRF-4. In order to account for the sequence preference of IRF-4, we focused on structural properties of DNA duplexes recognized by IRF-4. Here, we performed solution NMR studies on DNA duplexes containing GGGAAA and CCGAAA sequences, and assigned most of proton resonances of DNA 17 mer with GGGAAA. ^{1}H-^{1}H NOESY spectra indicated B-form like structure for GGGAAA. We also assigned imino proton resonances of DNA 17 mer with CCGAAA. For the imino proton region, the ^{1}H-^{1}H NOESY spectra of these two DNA duplexes were similar.

INTRODUCTION

IRF-4 is a lymphoid and myeloid restricted member of the IRF transcriptional family.[1,2] IRF family members bind to a consensus DNA-binding sequence, NNGAAA.[2] The crystal structure of PU.1/IRF-4/DNA (GTGAAA) ternary complex has been determined. This structure revealed that the kinked DNA structure is induced at the NN region, but the NN region of DNA does not interact with IRF-4 directly.[3] On the other hand, DNA sequences preferred by IRF-4 were determined by the selected amplified binding sequence (SABB) method, and they contained CCGAAA consensus sequence.[4]

Our isothermal titration calorimetry (ITC) experiments revealed that the DNA duplex containing CCGAAA sequence has higher affinity for IRF-4 than that containing GGGAAA sequence (Kojima et al., unpublished results). In order to account for the sequence preference of IRF-4, we focused on the structural properties of the DNA duplexes containing CCGAAA and GGGAAA sequences. Here, in order to investigate the structural properties of the DNA duplexes containing GGGAAA and CCGAAA sequences, we performed solution NMR studies on these DNA duplexes.

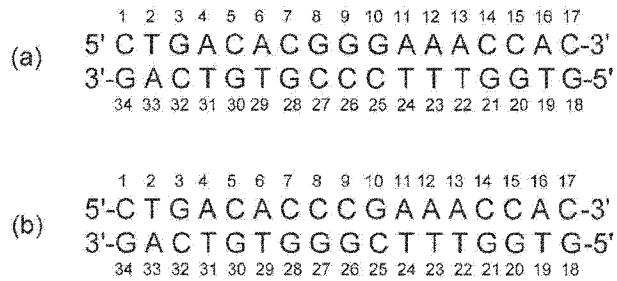

Scheme 1 Sequences of DNA duplexes containing GGGAAA (a) and CCGAAA (b).

RESULTS AND DISCUSSION

DNA oligomers (Scheme 1) were purchased from Fasmac Corp. (Atsugi, Japan), and NMR samples were prepared at the concentration of about 3 mM DNA duplexes in 90%/10% H_2O/D_2O containing 50 mM sodium phosphate (pH6.7), 100 mM sodium chloride, 0.1 mM EDTA, and 1 mM DTT. ^{1}H-^{1}H NOESY spectra of each DNA duplex were recorded with 30, 100, and 200 msec mixing times. DQF-COSY and TOCSY spectra of each DNA duplex were also recorded. All NMR spectra were recorded at 303 K on a Bruker DRX800 spectrometer.

For the DNA duplex containing GGGAAA sequence, we obtained nearly complete proton resonance assignments with the exception of H4', H5'/H5'', and NH_2 of A and G. Sequential connectivities between imino protons and between base H6/H8 and suger H1' protons are shown in Figure 1a and 1b, respectively, for ^{1}H-^{1}H NOESY spectra of the DNA duplex containing GGGAAA sequence. These NOESY spectra indicated that the DNA duplex containing GGGAAA sequence had B-form like structure. For the DNA duplex containing CCGAAA sequence, we assigned imino proton resonances. Figure 2 shows sequential connectivities between imino protons in the ^{1}H-^{1}H NOESY

spectrum of the DNA duplex containing CCGAAA sequence. For the imino proton regions of the ^{1}H-^{1}H NOESY spectra, no remarkable difference was observed between the DNA duplexes containing GGGAAA and CCGAAA sequences, and no special feature was found. We will complete proton resonance assignments of the DNA duplex containing CCGAAA sequence, and more detailed analyses of the structural properties of the DNA duplexes will be done.

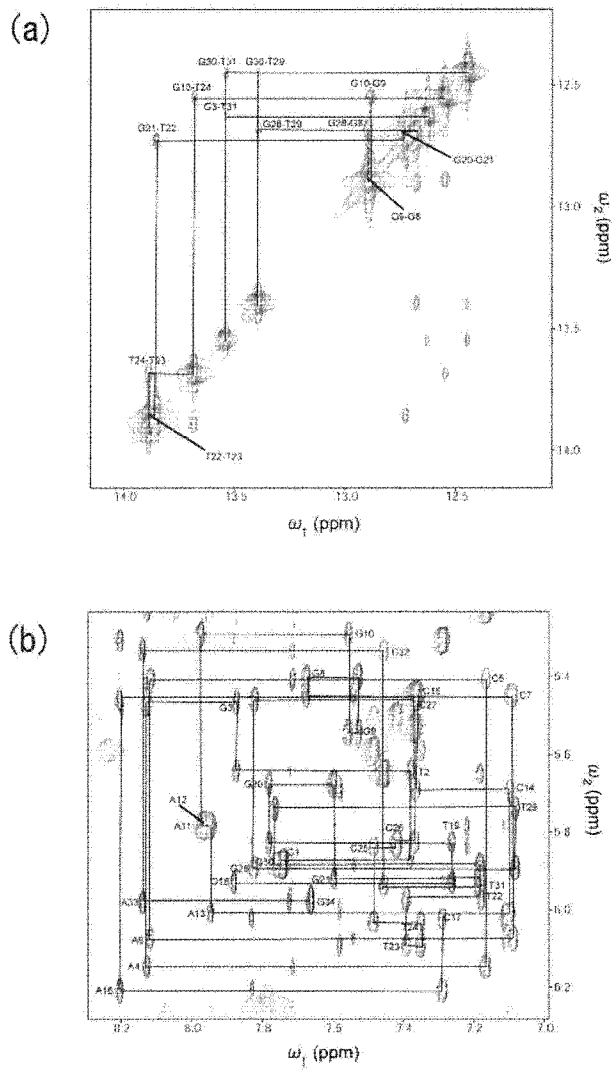

Figure 1 ^{1}H-^{1}H NOESY spectra of the DNA duplex containing GGGAAA sequence. (a) Imino proton region. Cross peaks between imino protons were labelled with residue numbers (ω_1-ω_2). The imino proton resonances 2, 18, 19, and 34 were not observed. (b) Base H6/H8 and suger H1' region. Intraresidue NOE cross peaks between H6/H8 and H1' were labelled with their residue numbers.

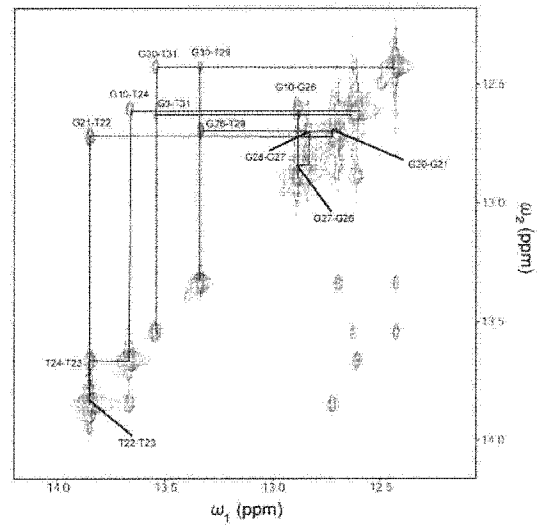

Figure 2 ^{1}H-^{1}H NOESY spectrum of the DNA duplex containing CCGAAA sequence. Imino proton region is shown. Cross peaks between imino protons were labelled with residue numbers (ω_1-ω_2). The imino proton resonances 2, 18, 19, and 34 were not observed.

CONCLUSION

We assigned most of proton resonances of the DNA duplex containing GGGAAA sequence, and imino proton resonances of the DNA duplex containing CCGAAA sequence. The DNA duplex containing GGGAAA sequence had B-form like structure. For the imino proton region, the ^{1}H-^{1}H NOESY spectra of these DNA duplexes were similar. These results suggest that both DNA duplexes have similar B-form like structure, and thus, the indirect DNA recognition mechanism of IRF-4 does not depend on the free DNA structure.

REFERENCES

1. Mittrucker, H. W., Matsuyama, T., Grossman, A., Kundig, T. M., Potter, J., Shahinian, A., Wakeham, A., Patterson, B., Ohashi, P. S. Mak, T. W. (1997) *Science*, **275**, 540-543.
2. Mamane, Y., Heylbroeck, C., Pierre, G., Algarte, M., Servant, M. J., LePage, C., DeLuca, C., Kwon, H., Lin, R., Hiscott, J. (1999) *Gene*, **237**, 1-14.
3. Escalante, C. R., Brass, A. L., Pongbala, J. M. R., Shatova, E., Shen, L., Singh, H. Aggarwal, A. K. (2002) *Mol. Cell*, **10**, 1097-1105.
4. Yoshida, K., Yamamoto, K., Kohno, T., Hironaka, N., Yasui, K., Kojima, C., Mukae, H., Kadata, J., Suzuki, S., Honma, K., Kohno, S., Matsuyama, T. (2005) *Int. Immunol.*, **17**, 1463-1471.

J|A|C|S
COMMUNICATIONS

Published on Web 12/21/2006

$^{15}N-^{15}N$ *J*-Coupling Across Hg^{II}: Direct Observation of Hg^{II}-Mediated T−T Base Pairs in a DNA Duplex

Yoshiyuki Tanaka,*,† Shuji Oda,† Hiroshi Yamaguchi,† Yoshinori Kondo,† Chojiro Kojima,‡ and Akira Ono*,§

Graduate School of Pharmaceutical Sciences, Tohoku University, Aobayama, Aoba-ku, Sendai, Miyagi 980-8578, Japan, Graduate School of Biological Sciences, Nara Institute of Science and Technology, Ikoma, Nara 630-0101, Japan, and Department of Material and Life Chemistry, Faculty of Engineering, Kanagawa University, 3-27-1 Rokkakubashi, Kanagawa-ku, Yokohama, Kanagawa 221-8686, Japan

Received August 1, 2006; E-mail: tanaka@mail.pharm.tohoku.ac.jp; akiraono@kanagawa-u.ac.jp

Recently, nucleic acid-metal interactions are recognized as an important topic to be solved,[1] as they are involved in RNA folding, mechanisms of ribozymes action, gene mutations (Hg^{II}-induced mutation[2]) and the design of biomolecular devices with metal cofactors. Therefore, metal-mediated base pairs with "artificial" bases have been extensively studied for use in nanodevices and as tools for biotechnology.[3] By contrast, we have previously reported that a "natural" base, thymine−thymine (T−T) mismatch in a DNA duplex, specifically binds to Hg^{II} [4] and applied this property to a Hg^{II}-sensor.[5] In addition, these studies revealed that the putative Hg^{II}-mediated T−T base pair (T−Hg^{II}−T pair) is at least as stable as normal Watson−Crick base pairs. Therefore, the chemical structure of the T−Hg^{II}−T pair is an interesting target to understand the Hg^{II}-specificity and the stability of the T−Hg^{II}−T pair.

Although several groups have studied Hg^{II}-thymine binding and a possible structure of T−Hg^{II}−T pairs (Figure 1a),[6] no definitive conclusion has been made until now. In the present study, we determined the chemical structure of the T−Hg^{II}−T pair, on the basis of ^{15}N NMR studies in which novel $^{15}N-^{15}N$ *J*-coupling across Hg^{II} ($^2J_{NN}$) was observed for this T−Hg^{II}−T pair, and this *J*-coupling ($^2J_{NN}$) is a direct evidence for the formation of T−Hg^{II}−T pairs.

Recently, we and other groups have reported that ^{15}N NMR chemical shift changes[7−10] are applicable to the detection of hydrogen-bond formations and RNA metallations, and $^{15}N-^{15}N$ *J*-coupling across a hydrogen bond ($^{2h}J_{NN}$)[11,12] is a definitive method to detect hydrogen bonds (Figure S1 in Supporting Information). Therefore, we postulated that the following NMR techniques with advanced ^{15}N NMR spectroscopy might be applicable for the determination of the chemical structure of the T−Hg^{II}−T pair, in combination with recently developed DNA labeling techniques: (1) Metal ion-binding sites could be specified by ^{15}N NMR chemical shift changes and (2) $^{15}N-^{15}N$ *J*-coupling across a metal center ($^2J_{NN}$) (Figure 1a) might reveal the pairing mode and partners in T−Hg^{II}−T pairs (N−Hg^{II}−N bond connectivity). Therefore, in the current study, we tried to detect $^2J_{NN}$ and chemical shift changes, by using ^{15}N NMR spectroscopy (Figure 2).

For the detection of $^2J_{NN}$, ^{15}N-labeled DNA oligomers **1**−**4** were chemically synthesized (Figure 1c).[12a] We then examined the stability of this duplex in the presence of Hg^{II}, and found that this duplex was stable enough for NMR analyses (T_m = 54 °C: Figures S2−S5 in Supporting Information). As the first trial, we measured the ^{15}N NMR spectrum of duplexes **1**•**3** with ^{15}N-labeled thymidines (T5 and T16) (Figure 2a). Notably, we clearly observed splitting

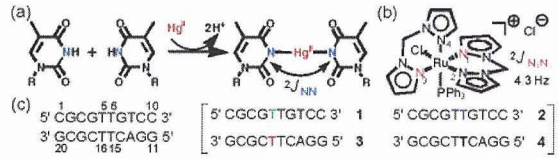

Figure 1. T−Hg^{II}−T pair and DNA oligomers. (a) Suggested base-pairing mode of the T−Hg^{II}-T pair and putative *J*-coupling of ^{15}N−Hg^{II}−^{15}N bond ($^2J_{NN}$). (b) Hexacoordination Ru^{II}-complex ($[RuCl(PPh_3)(BPM)_2]^+ \bullet Cl^-$) and *J*-coupling across Ru^{II} ($^2J_{N1N3}$) (see also Figure S1 in Supporting Information). (c) DNA oligomers with a ^{15}N-labeled thymidine at N3. Oligomers are named sequentially. Labeled thymidines are colored in terms of their positions.

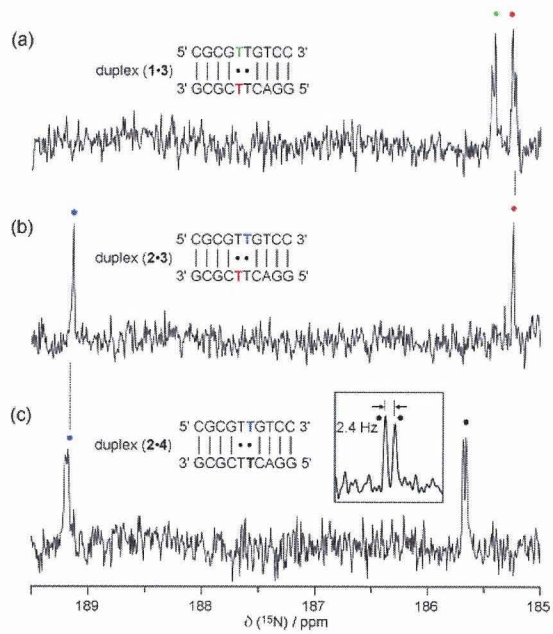

Figure 2. One-dimensional (1D) ^{15}N NMR spectra of duplex−Hg^{II} (1:2) complexes are shown: (a) the spectrum of the duplex (**1**•**3**)−Hg^{II} complex; (b) the spectrum of the duplex (**2**•**3**)−Hg^{II} complex; (c) the spectrum of the duplex (**2**•**4**)−Hg^{II} complex. The inset of the panel c indicates the resolution enhanced spectrum of the N3 resonance of T16 [N3(T16)]. The coupling constant of ^{15}N−Hg^{II}−^{15}N ($^2J_{NN}$) is shown in Hz as an absolute value. N3 resonances of thymidines are labeled with colored circles. Each color represents the position of the residue. ^{15}N-frequency (0 ppm) is 81.07646745 MHz.

of ^{15}N resonances for duplex **1**•**3**, most likely *J*-couplings ($^2J_{NN}$) (Figure 2a) which suggests the formation of a T5−Hg^{II}−T16 pair. Next, in duplex **2**•**4**, splitting of ^{15}N resonances was observed as well (a possible $^2J_{NN}$ for T6−Hg^{II}−T15 pair) (Figure 2c). By

† Tohoku University.
‡ Nara Institute of Science and Technology.
§ Kanagawa University.

10.1021/ja065552h CCC: $37.00

Table 1. Table of ^{15}N Chemical Shift Values[a]

atom[b]	metal	free	complex	difference
N3(T5)	Hg^{II}	155.1	185.4	+30.3
N3(T6)	Hg^{II}	153.9	189.2	+35.3
N3(T15)	Hg^{II}	155.8	185.7	+29.9
N3(T16)	Hg^{II}	154.4	185.2	+30.8

[a] Chemical shifts are listed in ppm. The "difference" is ^{15}N chemical shift difference between metal-free and metalated forms. [b] N3(T5), N3(T6), N3(T15) and N3(T16) denote the N3 atoms in the T5, T6, T15, and T16 residues, respectively. See also Tables S2 and S3, and Figure S6 in Supporting Information for further details.

contrast, these splittings disappeared for duplex **2•3** in which labeled thymidines are base-paired with nonlabeled thymidines (Figure 2b). Accordingly, Figure 2b demonstrates that the splitting of ^{15}N resonances observed in duplexes **1•3** and **2•4** (Figure 2a,c) truly rose from *J*-coupling ($^2J_{NN}$). In addition, we can assign all the N3 resonances in T−Hg^{II}−T pairs by using spectra of these combinations of the labeled duplexes. At this stage, we can conclude that T5−Hg^{II}−T16 and T6−Hg^{II}−T15 pairs were surely formed. As a result, our ^{15}N NMR data demonstrate that two imino protons are released upon T−Hg^{II}−T pairing (Figure 1a), which is a novel metal ion-binding manner for DNA and RNA molecules.

For the detailed analysis of the $^2J_{NN}$ value, we compared the $^2J_{NN}$ value with those of other related compounds. As a reference compound, there is a Ru^{II}-complex with a hexa-coordinated octahedral geometry (Figure 1b). In this complex, $^2J_{NN}$ for ^{15}N−Ru^{II}−^{15}N bonds was 4.3 Hz.[13] Unfortunately, there are currently limited data available on $^2J_{NN}$ across a metal center, and it is difficult to determine the relationship between the chemical structure and these *J*-coupling values. However, it is interesting that $^2J_{NN}$ for ^{15}N−Ru^{II}−^{15}N is in the same order to those for the T−Hg^{II}−T pairs (2.4 Hz) (Figure 2, Figure S1, and Table S1 in Supporting Information).

For the characterization of N−Hg^{II}−N bonds, we investigated the ^{15}N chemical shift perturbations upon the N−Hg^{II}−N bond formation (Table 1) (See also Figures S6 and S7 and Tables S2 and S3 in Supporting Information). All N3 resonances in the metal-free form were assigned from ^1H-^{15}N HSQC spectra of duplexes **1•3**, **2•4**, and **2•3** (see Figure S7 for assignment details). It was found that huge lower-field shifts of N3 resonances (approximately 30 ppm) were observed upon the N−Hg^{II}−N bond formation (Table 1). Such lower-field shifts cannot be explained without drastic transformations such as proton−Hg^{II} exchanges upon T−Hg^{II}−T pairing. Interestingly, in the cases of other proton−metal exchange systems, such as pyrrole−metal complexations, lower-field shifts of ^{15}N resonances upon metallations were observed (Figures S6 and Table S2 in Supporting Information). Therefore, the ^{15}N chemical shift changes for the T−Hg^{II}−T pairing and the related complexations exhibited lower-field shifts, which is sharp contrast to the higher-field shift of the $^{15}N7$(guanosine) upon its innersphere coordination to Cd^{II}, Zn^{II}, and Hg^{II}.[9,10]

Although NMR studies on the Hg^{II}−DNA interaction have been reported,[14] we emphasize that our data are the first definitive determination of the chemical structure of T−Hg^{II}−T pairs, as well as the first ^{15}N NMR data on the direct interaction site (N3 of thymidine) of Hg^{II}. Therefore, our results are the most rigorous and provide a definitive answer for its chemical structure. Furthermore, even in the cases of metal-complexes, ^{15}N NMR data on N-metal bonds are rare and we now provide the first ^{15}N NMR data of N−Hg^{II}−N bonds. Therefore, our observations are not only important data for nucleic acid-metal systems but also provide a fundamental basis for coordination chemistry.

In conclusion, we have demonstrated that $^2J_{NN}$ across a metal center is observable in a biological macromolecule (DNA duplex) and definitely determined the chemical structure of the T−Hg^{II}−T pair by using $^2J_{NN}$. We then found a novel metal ion-binding mode for DNA molecules, which includes the imino proton−metal exchange processes.

Hazardous Information. For safety, it is recommended that $Hg(ClO_4)_2$ should be handled with gloves.

Acknowledgment. This work was supported by a Grant-in-Aid for Scientific Research (C) (18550146) (for Y.T.), Scientific Research (B) (16350090) (for A.O.) and the "Scientific Frontier" Project (2006-2011) (for A.O.) from the Ministry of Education, Culture, Sports, Science and Technology, Japan, and The Mitsubishi Foundation (for A.O.).

Supporting Information Available: Experimental section; tables of *J*-coupling values, chemical shifts, and their perturbations; figures of metal-complexes (chemical shift) and their *J*-coupling; ^1H−^{15}N HSQC spectra; thermal denaturation profiles. This material is available free of charge via the Internet at http://pubs.acs.org.

References

(1) Lippard, S. J.; Berg, J. M. *Principles of Bioinorganic Chemistry*, University Science Books: Mill Valley, CA, 1996.
(2) Ariza, M. E.; Williams, M. V. *J. Biochem. Mol. Toxicol.* **1999**, *13*, 107−112.
(3) (a) Meggers, E.; Holland, P. L.; Tolman, W. B.; Romesberg, F. E.; Schultz, P. G. *J. Am. Chem. Soc.* **2000**, *122*, 10714−10715. (b) Weizman, H.; Tor, Y. *J. Am. Chem. Soc.* **2001**, *123*, 3375−3376. (c) Tanaka, K.; Tengeiji, A.; Kato, T.; Toyama, N.; Shionoya, M. *Science* **2003**, *299*, 1212−1213. (d) Switzer, C.; Sinha, S.; Kim, P. H.; Heuberger, B. D. *Angew. Chem., Int. Ed.* **2005**, *44*, 1529−1532. (e) The references cited therein.
(4) (a) Miyake, Y.; Togashi, H.; Tashiro, M.; Yamaguchi, H.; Oda, S.; Kudo, M.; Tanaka, Y.; Kondo, Y.; Sawa, R.; Fujimoto, T.; Machinami, T.; Ono, A. *J. Am. Chem. Soc.* **2006**, *128*, 2172−2173. (b) Tanaka, Y.; Yamaguchi, H.; Oda, S.; Nomura, M.; Kojima, C.; Kondo, Y.; Ono, A. *Nucleosides, Nucleotides Nucleic Acids* **2006**, *25*, 613−624.
(5) Ono, A.; Togashi, H. *Angew. Chem., Int. Ed.* **2004**, *43*, 4300−4302.
(6) (a) Yamane, T.; Davidson, N. *Biochim. Biophys. Acta* **1962**, *55*, 780−782. (b) Katz, S. *Biochim. Biophys. Acta* **1963**, *68*, 240−253. (c) Simpson, R. B. *J. Am. Chem. Soc.* **1964**, *86*, 2059−2065. (d) Kosturko, L. D.; Folzer, C.; Atewart, R. T. *Biochemistry* **1974**, *13*, 3949−3952. (e) Gruenwedel, D. W.; Cruikshank, M. K. *Biochemistry* **1990**, *29*, 2110−2116.
(7) (a) Zhang, X.; Gaffney, B. L.; Jones, R. A. *J. Am. Chem. Soc.* **1998**, *120*, 6625−6626 and references cited therein.
(8) (a) Tanaka, Y.; Kojima, C.; Yamazaki, T.; Kodama, T. S.; Yasuno, K.; Miyashita, S.; Ono, A.; Ono, A.; Kainosho, M.; Kyogoku, Y. *Biochemistry* **2000**, *39*, 7074−7080.
(9) (a) Tanaka, Y.; Kojima, C.; Morita, E. H.; Kasai, Y.; Yamasaki, K.; Ono, A.; Kainosho, M.; Taira, K. *J. Am. Chem. Soc.* **2002**, *124*, 4595−4601. (b) Tanaka, Y.; Kasai, Y.; Mochizuki, S.; Wakisaka, A.; Morita, E. H.; Kojima, C.; Toyozawa, A.; Kondo, Y.; Taki, M.; Takagi, Y.; Inoue, A.; Yamasaki, K.; Taira, K. *J. Am. Chem. Soc.* **2004**, *126*, 744−752. (c) Tanaka, Y.; Taira, K. *Chem. Commun.* **2005**, 2069−2079.
(10) (a) Wang, G.; Gaffney, B. L.; Jones, R. A. *J. Am. Chem. Soc.* **2004**, *126*, 8908−8909. (b) Fan, Y.; Gaffney, B. L.; Jones, R. A. *J. Am. Chem. Soc.* **2005**, *127*, 17588−17589.
(11) Dingley, A. J.; Grzesiek, S. *J. Am. Chem. Soc.* **1998**, *120*, 8293−8297.
(12) (a) Pervushin, K.; Ono, A.; Fernández, C.; Szyperski, T.; Kainosho, M.; Wüthrich, K. *Proc. Natl. Acad. Sci. U.S.A.* **1998**, *95*, 14147−14151. (b) Kojima, C.; Ono, A.; Kainosho, M. *J. Biomol. NMR* **2000**, *18*, 269−277. (c) Ishikawa, R.; Kojima, C.; Ono, A.; Kainosho, M. *J. Magn. Reson.* **2001**, *39*, S159−S165.
(13) (a) Otting, G.; Messerle, B. A.; Soler, L. P. *J. Am. Chem. Soc.* **1997**, *119*, 5425−5434. (b) Otting, G.; Soler, L. P.; Messerle, B. A. *J. Magn. Reson.* **1999**, *137*, 413−429.
(14) (a) Young, P. R.; Nandi, U. S.; Kallenbach, N. R. *Biochemistry* **1974**, *13*, 3949−3952. (b) Kuklenyik, Z.; Marzilli, L. G. *Inorg. Chem.* **1996**, *35*, 5654−5662. (c) Onyido, I.; Norris, A. R.; Buncel, E. *Chem. Rev.* **2004**, *104*, 5911−5929. (d) The references cited therein.

JA065552H

THE JOURNAL OF BIOLOGICAL CHEMISTRY VOL. 282, NO. 4, pp. 2741–2751, January 26, 2007

Solution Structure of the Cytoplasmic Region of Na^+/H^+ Exchanger 1 Complexed with Essential Cofactor Calcineurin B Homologous Protein 1*[S]

Received for publication, April 28, 2006, and in revised form, October 6, 2006 Published, JBC Papers in Press, October 18, 2006, DOI 10.1074/jbc.M604092200

Masaki Mishima[‡], Shigeo Wakabayashi[§], and Chojiro Kojima[‡1]

From the [‡]Graduate School of Biological Sciences, Nara Institute of Science and Technology, Ikoma, Nara 630-0192, Japan and [§]Department of Molecular Physiology, National Cardiovascular Center Research Institute, Suita, Osaka 565-8565, Japan

Na^+/H^+ exchanger 1 (NHE1) regulates intracellular pH, Na^+ content, and cell volume. Calcineurin B homologous protein 1 (CHP1) serves as an essential cofactor that facilitates NHE1 exchange activity under physiological conditions by direct binding to the cytoplasmic juxtamembrane region of NHE1. Here we describe the solution structure of the cytoplasmic juxtamembrane region of NHE1 complexed with CHP1. The region of NHE1 forms an amphipathic helix, which is induced by CHP1 binding, and CHP1 possesses a large hydrophobic cleft formed by EF-hand helices. The apolar side of the NHE1 helix participates in extensive hydrophobic interactions with the cleft of CHP1. We suggest that helix formation of the cytoplasmic region of NHE1 by CHP1 is a prerequisite for generating the active form of NHE1. The molecular recognition detailed in this study also provides novel insight into the target binding mechanism of EF-hand proteins.

Na^+/H^+ exchangers comprise a family of countertransport proteins that catalyze the electroneutral exchange of Na^+ and H^+. Nine isoforms of the Na^+/H^+ exchanger have been isolated and shown to possess similar membrane topologies consisting of 12 N-terminal membrane-spanning helices and a large C-terminal cytoplasmic region (Fig. 1*A*). The exchanger isoforms exhibit tissue-specific expression, membrane localization, and kinetic and pharmacological properties (1). They participate in a broad range of physiological processes including the regulation of cell volume, transepithelial transport of electrolytes, cell proliferation, apoptosis, and differentiation. Isoforms NHE1–5, localized at the plasma membrane, are primarily involved in the regulation of intracellular pH (pH_i)[2] and Na^+ concentration (1).

Of them, the ubiquitously expressed isoform NHE1 is the best studied mammalian Na^+/H^+ exchanger. The activity is controlled by various extrinsic factors including hormones, growth factors, pharmacological agents, and mechanical stimuli (1). The regulation of NHE1 by these external stimuli is thought to be exerted through the action of a variety of signaling molecules including calcineurin B homologous protein (2, 3), calmodulin (4, 5), low molecular mass GTPases of the Ras and Rho family (6–8), p42/44 mitogen-activated protein kinases (9), p90 ribosomal S6 kinase (10), 14-3-3 protein (11), Nck-interacting kinase (12), and phosphatidylinositol 4,5-bisphosphate (13). However, the detailed mechanism through which these events occur remains unknown.

Among these factors, CHP1 can serve as an essential cofactor and is required by at least three NHE isoforms (NHE1–3) to express high physiological levels of exchange activity (3). It was shown that CHP1 bound directly to the juxtamembrane region of the C-terminal cytoplasmic domain. When GFP-CHP1 and NHE1–3 were co-expressed, it was found that GFP-CHP1 was mostly localized at the cell surface, whereas co-expression of CHP1 and a CHP1 binding-defective NHE1 mutant failed to show co-localization, implying that NHE1 is a principal target of CHP1 (3). In addition to reduced activity in the neutral pH range, the CHP1 binding-defective NHE1 mutant showed a marked reduction in pH_i sensitivity (~0.7 pH unit acidic shift) that subsequently abolished various NHE1 regulatory responses. Furthermore CHP1 deprivation resulted in marked reduction (>90%) of NHE1 activity (3). These observations suggest that the association of NHE1 with CHP1 is critical for activity and the maintenance of NHE1 pH_i sensitivity (14).

CHP1 consists of four EF-hands, the primary sequence of which is homologous to calmodulin (CaM) and calcineurin B

* This work was supported in part by grants-in-aid for Scientific Research on Priority Area and the 21st Century of Excellence (COE) Program from the Ministry of Education, Culture, Sports, Science and Technology (MEXT), Japan (to M. M. and C. K.), and Grant nano-001 for Research on Advanced Medical Technology from the Ministry of Health, Labor and Welfare of Japan and Grant-in-aid for Priority Areas 13142210 for Scientific Research from the MEXT (to S. W.). The costs of publication of this article were defrayed in part by the payment of page charges. This article must therefore be hereby marked "*advertisement*" in accordance with 18 U.S.C. Section 1734 solely to indicate this fact.

[S] The on-line version of this article (available at http://www.jbc.org) contains supplemental Table S1 and Figs. S2 and S3.

The atomic coordinates and structure factors (code 2E30) have been deposited in the Protein Data Bank, Research Collaboratory for Structural Bioinformatics, Rutgers University, New Brunswick, NJ (http://www.rcsb.org/).

[1] To whom correspondence should be addressed: Graduate School of Biological Sciences, Nara Institute of Science and Technology, 8916-5 Takayama, Ikoma, Nara 630-0192, Japan. Tel.: 81-743-72-5571; Fax: 81-743-72-5579; E-mail: kojima@bs.naist.jp.

[2] The abbreviations used are: pH_i, intracellular pH; HSQC, heteronuclear single quantum coherence; NOE, nuclear Overhauser effect; NOESY, NOE spectroscopy; TOCSY, total correlation spectroscopy; CANDID, combined automated NOE assignment and structure determination module; CaM, calmodulin; CNB, calcineurin B; NHE, Na^+/H^+ exchanger; CHP, calcineurin B homologous protein; CNA, calcineurin A; Ni-NTA, nickel-nitrilotriacetic acid; GST, glutathione *S*-transferase; CHAPS, 3-[(3-cholamidopropyl)dimethylammonio]-1-propanesulfonic acid; r.m.s., root mean square; Kv, voltage-gated potassium channel; KChIP, Kv-interacting protein; PIP_2, phosphatidylinositol 4,5-bisphosphate.

Supplemental Material can be found at: http://www.jbc.org/cgi/content/full/M604092200/DC1

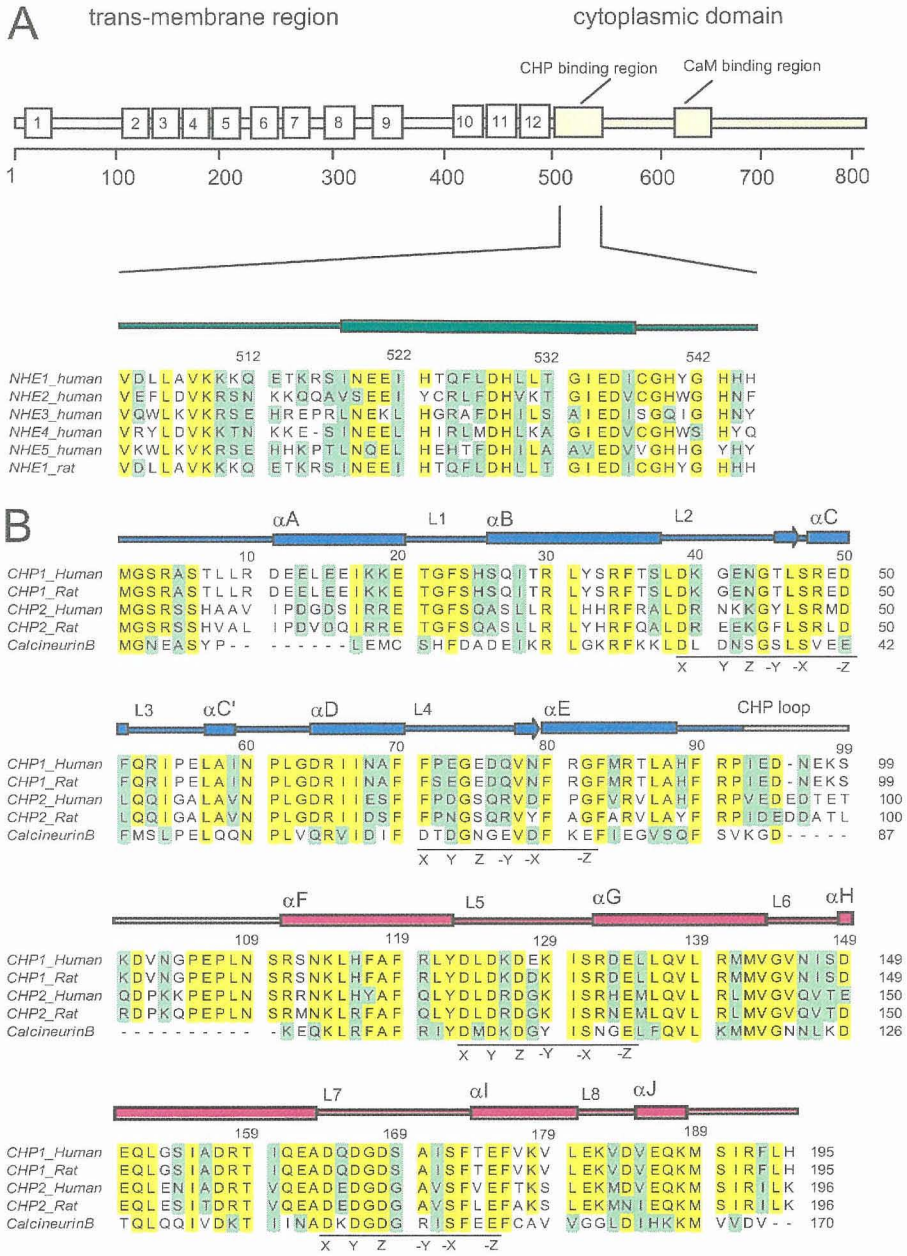

FIGURE 1. **Multiple sequence alignments of NHE1 and CHP1.** *A*, domain structure and alignment of NHE1. *B*, alignment of CHP1, CHP2, and human calcineurin B. In *A* and *B*, sequence alignment was performed using ClustalW. Secondary structure elements of the proteins are shown schematically at the *top* of the alignments. N- and C-terminal domains of CHP1 are colored in *blue* and *magenta*, respectively, for clarity. Conserved and semiconserved residues are colored in *yellow* and *green*, respectively. The 12-residue motif involved in the EF-hand is *underlined*, and key residues are indicated as *X*, *Y*, *Z*, *-Y*, *-X*, and *-Z*.

(CNB), possessing 31 and 41% sequence identity, respectively (Fig. 1*B*). It is well known that all CaM and CNB EF-hands can bind Ca^{2+}. However, CHP1 EF-1 and EF-2 are ancestral and do not bind Ca^{2+} under physiological conditions, whereas EF-3 and EF-4 bind two Ca^{2+} ions with high affinity (~90 nM) based on the $^{45}Ca^{2+}$ binding experiments for several CHP1 mutants (14). Complex formation between CHP1 and the CHP1 binding domain of NHE1 resulted in a marked increase in Ca^{2+} binding affinity (K_d = ~2 nM) (14). This suggests that CHP1 constitutively contains two Ca^{2+} ions when associated with NHE1 in cells (14).

Interestingly CHP1 has been reported to exhibit multiple functions. It was initially identified as a protein (p22) involved in vesicular transport (15) and the inhibition of calcineurin phosphatase activity (16). It was also found to interact with microtubules (17), DRAK2 (death-associated protein kinase-related apoptosis-inducing protein kinase 2) (18) and KIF1Bβ2 (kinesin family 1Bβ2) (19).

A second CHP isoform, CHP2, with 61% sequence identity was also identified and found to be involved in the maintenance of abnormally high pH_i in malignantly transformed cells. CHP2 is expressed at a relatively high level in malignantly transformed cells and in rat small intestine, suggesting that it plays a specific role in this tissue (20). In addition, tescalcin, an EF-hand protein closely related to CNB, that interacts with the cytoplasmic region of NHE1 has been identified (21, 22).

The crystal structure of NHE1-unbound rat CHP1 was recently determined and revealed that the overall structure is similar to CNB where Ca^{2+} ions are coordinated within EF-3 and EF-4. However, the interaction mechanism between NHE1 and CHP1 remains unknown (23).

Here we report on the solution structure of the cytoplasmic region of NHE1 bound to CHP1 as determined by NMR. Details of the NHE1-CHP1 interaction are described. We present mutational binding data to delineate the significance of the interactions observed in the complex. Based on the structure, we suggest a role for CHP1 in terms of NHE1 activation. Comparisons of the binding mode between NHE1-CHP1 and calcineurin A (CNA), CNB, and other related four-EF-hand proteins are also discussed.

EXPERIMENTAL PROCEDURES

Sample Preparation—The NHE1-CHP1 complex was co-expressed and co-purified. DNA encoding NHE1 was cloned into the pET24a vector (Novagen), and CHP1 was subcloned into pET11a (Novagen), which produces recombinant protein with a hexahistidine (His_6) sequence at the C terminus. The proteins were co-overexpressed in *Escherichia coli* BL21(DE3) cells. Uniformly ^{15}N- and $^{15}N/^{13}C$-labeled proteins were prepared by